

Novel *Drosophila* two-pore domain K⁺ channels: rescue of channel function by heteromeric assembly

Frank Döring,¹ Henrike Scholz,² Ronald P. Kühnlein,³ Andreas Karschin¹ and Erhard Wischmeyer¹

¹Institute of Physiology, University of Würzburg, Röntgenring 9, 97070 Würzburg, Germany

²Theodor-Boveri Institute, Department of Genetics and Neurobiology, University of Würzburg, Am Hubland, 97074 Würzburg, Germany

³Molecular Developmental Biology, Max-Planck Institute for Biophysical Chemistry, Am Fassberg 11, 37070 Göttingen, Germany

Keywords: background current, local anesthetics, olfactory learning, pH sensor, potassium channel genes

Abstract

Ten genes with essential structural features of two-pore domain potassium channels were identified in the genome of *Drosophila melanogaster*. Two *Drosophila* two-pore domain potassium subunits displayed substantial amino acid similarity to human TWIK-related acid-sensitive K⁺ (TASK) channels (38–43%), whereas all others were less than 26% similar to any human homolog. The cDNAs of *Drosophila* TASK (dTASK)-6 and dTASK-7 channels were isolated from adult fruit flies. In Northern blots dTASK transcripts were found predominantly in the head fraction of adult flies and whole-mount brain *in situ* hybridizations showed strongly overlapping expression patterns of both dTASK isoforms in the antennal lobes. When heterologously expressed in *Drosophila* Schneider 2 cells, dTASK-6 gave rise to rapidly activating K⁺-selective currents that steeply depended on external pH. Structural elements in the extracellular M1–P1 loop of dTASK-6 were found to be involved in proton sensation. In contrast to mammalian TASK channels, the pH sensitivity was independent of extracellular histidines adjacent to the GYG selectivity filter (His98). As revealed by mutational analysis, functional expression of dTASK-7 was prevented by two nonconserved amino acids (Ala92-Met93) in the pore domain. When these two residues were replaced by conserved Thr92-Thr93, typical K⁺-selective leak currents were generated that were insensitive to changes in external pH. Nonfunctional wildtype dTASK-7 channels appeared to form heteromeric assemblies with dTASK-6. Following cotransfection of dTASK-6 and wildtype dTASK-7 (or when engineered as concatemers), K⁺ currents were observed that were smaller in amplitude, harbored slower activation kinetics and were considerably less inhibited by local anesthetics as compared with dTASK-6. Thus, pore-loop residues in dTASK-7 changed functional and pharmacological properties in heteromeric dTASK channels.

Introduction

Two-pore domain potassium (K_{2P}) channels represent a family of background channels with functional properties consistent with a role in setting the membrane potential and input resistance of neurons. Although these background K⁺ channels show some constitutive activity at normal resting potential, they are also subject to modulation by numerous factors. For example, channel activity is influenced by relevant physicochemical conditions such as temperature, membrane stretch and intracellular or extracellular pH and can be modulated by neurotransmitters, bioactive lipids and anesthetics. Thus, K_{2P} channels are key molecules for sensory features of central and peripheral neurons, altering their excitability by extracellular stimuli (Patel & Honoré, 2001).

Mammalian K_{2P} channels contain four transmembrane segments (M1–M4) and two-pore forming domains (P1 and P2) in each subunit. It is believed that two subunits dimerize to form a K⁺-selective pore. In humans, 15 K_{2P} channel subunits (KCNK) have been identified (reviewed by Goldstein *et al.*, 2001) and, due to structural and functional characteristics, they are divided into several subfamilies:

(i) weak inward rectifiers TWIK-1, TWIK-2 and KCNK-7; (ii) acid-sensitive TWIK-related acid-sensitive K⁺ (TASK)-1, TASK-3 and TASK-5; (iii) lipid-sensitive and mechano-gated TREK-1, TREK-2 and TRAAK; (iv) alkaline-activated TALK-1, TALK-2 and acid-sensitive TASK-2; (v) halothane-inhibited THIK-1 and THIK-2; and (vi) TWIK-related spinal cord K⁺ channel (TRESK, Sano *et al.*, 2003).

When expressed in heterologous systems most mammalian K_{2P} subunits allowed a comprehensive characterization of their functional and pharmacological properties (Patel & Honoré, 2001). In addition, there are a few K_{2P} subunits, e.g. THIK-2 and TASK-5, that failed to generate K⁺-selective currents when recombinantly expressed (Karschin *et al.*, 2001; Rajan *et al.*, 2001).

Within the TASK channel subfamily, TASK-1 (KCNK-3) and TASK-3 (KCNK-9) represent the members that were found predominantly in brain (Karschin *et al.*, 2001; Medhurst *et al.*, 2001) and share a number of functional properties. TASK currents expressed in recombinant systems are K⁺ selective, instantaneous, independent of voltage and outwardly rectifying in physiological K⁺ solution (Bayliss *et al.*, 2003). As their name suggests, they are sensitive to changes in extracellular pH, and both are activated by alkalization and inhibited by acidification, although at different pH values (pK values for channel activity, 7.4 and 6.8 for TASK-1 and TASK-3, respectively). Proton sensitivity in both subunits was found to be dependent on an

Correspondence: Dr Frank Döring, as above.

E-mail: fdoering@mail.uni-wuerzburg.de

Received 13 January 2006, revised 3 August 2006, accepted 8 August 2006

extracellular histidine residue (His98) adjacent to the GYG selectivity filter (Rajan *et al.*, 2000; Lopes *et al.*, 2001). Although pH sensitivity is the best diagnostic test for TASK channel activity, several other pharmacological properties of TASK channels exist. They are activated by clinically relevant concentrations of inhalational anesthetics, e.g. halothane (Patel *et al.*, 1999), and the endocannabinoid anandamide was identified as a potent blocker of TASK channel activity (Maingret *et al.*, 2001). Less specific inhibition of TASK currents was observed with local anesthetics and arachidonic acid (Kindler & Yost, 2005).

A common but not universal feature among closely related potassium channel subunits is their ability to coassemble into functional ionic pores. Here, association of different subunits often leads to heteromeric channels with properties discrete from those of the constituent subunits. Recently, coassembly of TASK-1 and TASK-3 subunits was demonstrated in recombinant expression systems as well as in native neuronal tissues with altered functional properties (Czirják & Enyedi, 2002; Berg *et al.*, 2004).

A large number of K_{2P} channels have been found in many different species since the first K_{2P} channel from *Drosophila melanogaster* was identified (ORK1; Goldstein *et al.*, 1996).

Here we document the cloning and expression of novel *Drosophila* K_{2P} (dK_{2P}) channels. Taking structural features into account, the functional and pharmacological properties of two isoforms, *Drosophila* TASK (dTASK)-6 and dTASK-7, are described in detail.

Materials and methods

Molecular cloning

Using BLAST software, protein sequences of mammalian K_{2P} channel sequences were used to search for *Drosophila* homologs in both FlyBase (Drysdale *et al.*, 2005; <http://flybase.org/>) and the Celera genome database (Adams *et al.*, 2000). Eleven polypeptides with sequence similarities to K_{2P} channels were identified. Seven of these annotated gene products (dTASK-6/*CG9637*, dTASK-7/*CG9361*, ORK1/*CG1615*, *CG1688*, *CG10864*, *CG8713* and *CG9194*) were chosen to amplify the corresponding cDNAs by either reverse transcriptase polymerase chain reaction (PCR) from total RNA of adult fruit flies or PCR from full-length expressed sequence tag clones (ORK1/*RE26149*; *CG8713*/*RE21922* and *CG1688*/*GH04802*) supplied by ResGen (Huntsville, AL, USA). Specific primers covering the entire open reading frames (ORFs) were deduced from predicted transcripts released in FlyBase:

dTASK-6 (5'-ATGAAGAAACAAAATGTGCGCACG-3' and 5'-CTAGATGCGTATGGACAGC-3'),

dTASK-7 (5'-ATGAAGCGACAGAATGTCCG-3' and 5'-TCAG-ACGGAGGCTCGCTTCA-3'),

ORK1 (5'-ATGTCGCCGAATCGATGG-3' and 5'-GGAAACCTAACATCTTC-3'),

CG8713 (5'-CAAGACATGTCTCCCGACGCA-3' and 5'-TAA-TTAGCTCCTAGGAGG-3'),

CG1688 (5'-GCGATCATGTCCGACGTTGAG-3' and 5'-GGATGAGCACATTATCCATC-3'),

CG10864 (5'-ATGGCCAGCAAATTCAGAGG-3' and 5'-CTAG-TAGTAATCATCCTC-3') and

CG9194 (5'-ATGTCGGGTAGGCGGGCCCAATC-3' and 5'-CT-AATCCTCATCCTGCTCGTC-3').

The cDNAs of entire ORFs were cloned into pSGEM and pAc5.1 (Invitrogen, Groningen, Netherlands) for functional expression in *Xenopus* oocytes and *Drosophila* Schneider 2 (S2) cells, respectively. DNA fragments used to label specific probes for northern blots and

in situ hybridizations were cloned into pCR-TOPO (Invitrogen). To assemble concatemers of both dTASK isoforms the stop codon of dTASK-6 was substituted by three alanine codons that were joined to the start ATG of dTASK-7 cDNA. The junction was generated by using the 'geneSOEing' technique (Horton *et al.*, 1989), which links two DNA fragments by sequential PCRs with overlap extension of PCR primers.

Single-strand cDNA was amplified with reverse transcriptase Super-script III (Invitrogen) and PCR fragments for cDNA cloning and concatemer construction were generated with *Taq* polymerase (Qiagen, Hilden, Germany) or *Pfu* polymerase (Stratagene, La Jolla, CA, USA).

For introduction of point mutations we used the QuikChange Mutagenesis Kit (Stratagene) according to the manufacturer's instructions. All PCR products, concatemers, chimeras and mutants were sequenced on both strands on an ABI Prism 310 Genetic Analyzer (Applied Biosystems, Weiterstadt, Germany). DNA analysis and sequence alignments (ClustalW algorithm) were performed with LASERGENE software (DNASTar, Madison, WI, USA).

Northern blot and in situ hybridization

Drosophila melanogaster strain Oregon R was reared on standard cornmeal-molasses-agar medium at 25 °C, and individuals of various developmental stages were collected and stored at -70 °C. Adult flies frozen in liquid nitrogen were vortexed and passed through a sieve to separate head and body fractions of the animal. Total RNA was isolated from 400–700 mg of frozen *Drosophila* stages either by RNeasy (Qiagen) (embryos, larvae and pupae) or WAK-Chemie TRI Reagent (adult flies). For northern blots 1 µg poly A⁺ RNA purified by Oligotex (Qiagen) was separated on a denaturing agarose gel and transferred to BrightStar Plus nylon membranes (Ambion, Austin, TX, USA). Northern blots were probed with [³²P]-UTP-labeled antisense RNA specific for dTASK-6 (ORF positions, Met1-Ile408) and dTASK-7 (Met1-Val339). As control, blots were probed with antisense RNA of the ribosomal protein gene *RpL9* (Schmidt *et al.*, 1996). Labeling, hybridization and probe removal were performed with NorthernMax and Strip-EZ reagents (Ambion) according to the manufacturer's instructions.

In situ hybridizations of whole-mount adult *Drosophila* males (Canton S) were performed as described by Tautz & Pfeifle (1989). Fixed flies were probed with digoxigenin-labeled (Roche, Mannheim, Germany) antisense RNAs that were specific for dTASK-6 and dTASK-7. Corresponding sense RNA probes were used to control the specificity of hybridization signals.

Cell culture and transfection

The S2 cell line derived from late stage (20–24-h-old) *D. melanogaster* embryos (Schneider, 1972) was purchased from Invitrogen. S2 cells were grown in Schneider's *Drosophila* medium (Invitrogen) supplemented with 10% fetal bovine serum and 100 U/mL penicillin-streptavidin at 25 °C without CO₂. Modified calcium phosphate precipitation was used for transfection of S2 cells. Briefly, cells were plated (35-mm dish) in 3 mL complete medium 1 h before transfection. Plasmid DNA (19 µg) dissolved in 300 µL CaCl₂ (240 mM) was slowly mixed with 300 µL 2× Hanks' balanced salt solution buffer (280 mM NaCl, 50 mM HEPES, 1.5 mM Na₂HPO₄, pH 7.05), and the mixture was incubated for 30 min at room temperature and subsequently added to the cells. After 16 h the cells were washed with medium and analysed 40 h after transfection. Transfected cells were identified by coexpression of green fluorescent protein (2 µg enhanced green fluorescent protein-pAc5.1).

Electrophysiology

For expression of dK_{2P} channels in *Xenopus laevis* oocytes, capped run-off poly (A⁺) cRNA transcripts from linearized cDNA were synthesized and ~6 ng was injected into defolliculated oocytes. Oocytes were prepared as described previously (Methfessel et al., 1986) and incubated at 20 °C in ND96 solution (96 mM NaCl, 2 mM KCl, 1 mM MgCl₂, 1 mM CaCl₂, 5 mM HEPES, pH 7.4) supplemented with 100 µg/mL gentamicin and 2.5 mM sodium pyruvate. At 48 h after injection two electrode voltage-clamp measurements were performed with a Turbo Tec-10 C amplifier (npi, Tamm, Germany). Oocytes were placed in a small volume perfusion chamber with a

constant flow of ND96 or high K⁺ solution (96 mM KCl, 2 mM NaCl, 1 mM MgCl₂, 1 mM CaCl₂, 5 mM HEPES, pH 7.4).

Whole-cell recordings of S2 cells were performed at room temperature 48 h after transfection in a bath solution consisting of 135 mM NaCl, 5.4 mM KCl, 1.8 mM CaCl₂, 1 mM MgCl₂, 10 mM glucose and 5 mM HEPES, pH 6.8. Patch pipettes were pulled from borosilicate glass capillaries (Kimble Products, Sussex, UK) and heat polished to give input resistances of 3–5 MΩ. The pipette recording solution contained 140 mM KCl, 0.01 mM CaCl₂, 2 mM MgCl₂, 1 mM EGTA, 1 mM Na₂ATP, 0.1 mM cAMP, 0.1 mM GTP and 5 mM HEPES, pH 7.3.

Currents were recorded from S2 cells with an EPC9 patch-clamp amplifier (Heka Electronics, Lambrecht, Germany). Stimulation and data acquisition were controlled by PULSE/PULSEFIT software (Heka Electronics) on a Macintosh computer, and data analysis was performed with IGOR software (WaveMetrics, Lake Oswego, OR, USA). Data were presented as means ± SD (number of cells). Series resistances were compensated automatically by the Heka Electronics software.

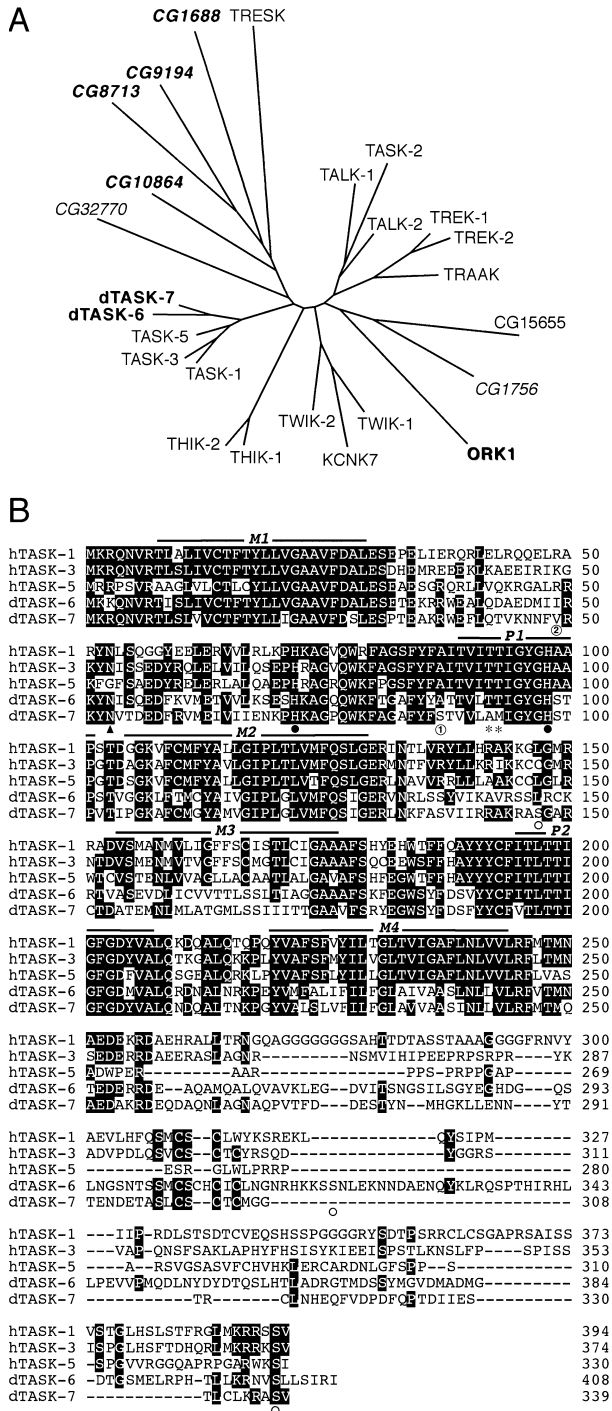
Results

Molecular characterization of two-pore domain potassium channels from Drosophila

Eleven putative K_{2P} channel genes were identified in the databases of Flybase and Celera by homology screening with conserved mammalian K_{2P} channel sequences. Ten annotated protein sequences revealed structural motifs typical of K_{2P} channels, i.e. two conserved pore forming domains (P1 and P2) each flanked by two transmembrane segments M1/M2 and M3/M4. The primary structure of one database entry (CG3367) displayed substantial similarity to K_{2P} channel sequences but only a single conserved pore forming domain surrounded by two transmembrane segments (Drysdale et al., 2005). Primers covering the entire ORFs were chosen to PCR amplify native cDNAs of dK_{2P} channels from various sources. For seven genes, a single transcript coding for a complete ORF was amplified (Fig. 1A, bold letters): dTASK-6, 1227 bp; dTASK-7, 1020 bp; ORK1, 3006 bp; CG8713, 1182 bp; CG1688, 2757 bp; CG10864, 1170 bp and CG9194, 2187 bp in length.

The predicted protein sequences of dK_{2P} channels varied in length from 339 to 1001 amino acids and the majority showed less than 26%

FIG. 1. Comparison of *Drosophila* two-pore domain potassium (K_{2P}) channels with their human orthologues. (A) Phylogenetic relationship as calculated from protein sequence alignments by ClustalW algorithm (LASERGENE software) and subsequently graphically converted with an 'unrooted' graphics program. *Drosophila* K_{2P} (dK_{2P}) channel subunits are represented by name, if functionally characterized [*Drosophila* TWIK-related acid-sensitive K⁺ (TASK) (dTASK)-6, dTASK-7 and ORK1], or by gene numbers assigned by the *Drosophila* genome project (e.g. CG1688). Bold lettering indicates channel subunits that were cloned and investigated in the present study. Human K_{2P} channels are depicted with their structural and functional nomenclature (e.g. TWIK-1). The dendrogram demonstrates that dTASK-6 and dTASK-7 are closely related to human TASK channels, whereas the other dK_{2P} channels apparently cannot be allocated to human K_{2P} channel subfamilies. (B) Similarities of dTASK-6 (GenBankTM Accession no. AJ920330) and dTASK-7 (AJ920331) with human orthologues TASK-1 (AF006823), TASK-3 (AF279809) and TASK-5 (AF294350) are shown by sequence alignment. Transmembrane segments (M1–M4) and pore forming domains (P1 and P2) are indicated by horizontal bars. Three and more identical amino acids are boxed in black. Nonconserved amino acids in the P1 region of dTASK-7 are marked by asterisks (*) and filled circles (●) indicate extracellular histidines investigated for acid sensitivity. Boundaries of chimeric constructs 1 and 2 are marked by encircled numbers. A consensus site for N-glycosylation present in the extracellular the M1–P1 linker of all TASK subunits is highlighted by an arrowhead. Three putative protein kinase A phosphorylation sites (K/R-K/R-X-S/T) in dTASK channels.



amino acid identity between each other as well as to their human homologs. Only the polypeptides of dTASK-6 (408 amino acids, GenBank™ Accession no. AJ920330) and dTASK-7 (339 amino acids, AJ920331) were 45% identical to each other and displayed between 38 and 45% amino acid identity to human TASK-1/3/5 subunits. The phylogenetic analysis revealed that human and *Drosophila* TASK subunits clustered on the same branch of the tree. Other dK_{2P} channels were located on separate branches indicating more distant phylogenetic relationships (Fig. 1A).

The alignment of human and *Drosophila* TASK subunits (Fig. 1B) demonstrated a high degree of sequence identity proximate to the plasma membrane but substantial amino acid variability, e.g. in the intracellular carboxy terminus. It is noteworthy that the intracellular amino termini of all TASK subunits were very short and highly conserved. In the extracellular MI–P1 linker a consensus site for N glycosylation was present in both dTASK subunits as well as in human TASK-1 and TASK-3 (arrowhead in Fig. 1B). Recognition sites for protein kinase A (PKA) phosphorylation were located in both dTASK subunits (open circles in Fig. 1B) but a carboxy-terminal site typical for mammalian TASK-1 and TASK-3 could only be found in the dTASK-7 subunit. Moreover, an alanine-methionine doublet was present in the P1 domain of dTASK-7 (asterisks in Fig. 1B) where two threonines were highly conserved within the K_{2P} channel family. dTASK-6 and dTASK-7 both harbored a six-amino-acid motif (VLR[F/M/L]T) next to transmembrane segment 4 that has been shown to serve important regulatory functions, e.g. control by G protein-coupled receptors in mammalian TASK channels (Talley & Bayliss, 2002).

Expression profile of *Drosophila* TASK channels

The expression profile of dTASK-6 and dTASK-7 was monitored at the transcript level during different developmental stages (Fig. 2A and B, lanes 1–5). For the dTASK-6 gene, a single transcript of ~4.5 kb was identified at all stages with increased amounts in pupa and a substantial reduction of transcripts in entire adult flies (Fig. 2A, lanes 1–5). To test for putative neuronal expression, head and body fractions of adult flies were analysed separately. Strong dTASK-6 expression was found in the head and almost no signal in the body (Fig. 2A, lanes 6 and 7). The dTASK-7 expression pattern as revealed by northern blots was very similar to the dTASK-6 profile. dTASK-7 transcripts (2.0 kb) were also most abundant in head fractions of adult flies and scarcely detectable in the body. Only in stage 3 larvae was the expression level of dTASK-7 significantly weaker compared with dTASK-6.

To determine whether strong signals in head fractions resulted from neuronal expression, fly brains were analysed by whole-mount *in situ* hybridizations. dTASK-6 and dTASK-7 transcripts were detected in the cortical region throughout the central region of the adult brain at various levels. Both were preferentially expressed in the cortex of the antennal lobes and no expression was observed in the optical lobes. Comparison of the brain expression patterns of dTASK-6 and dTASK-7 (Fig. 3A and B) indicated that they are likely to be colocalized in the same set of neurons.

Functional expression of two-pore domain potassium channels from *Drosophila*

After injection of ORK1 (Goldstein *et al.*, 1996) cRNA into *Xenopus* oocytes, large outwardly rectifying currents ($3.02 \pm 1.58 \mu\text{A}$ at +30 mV) were recorded in 2 mM external K⁺ using the two-electrode

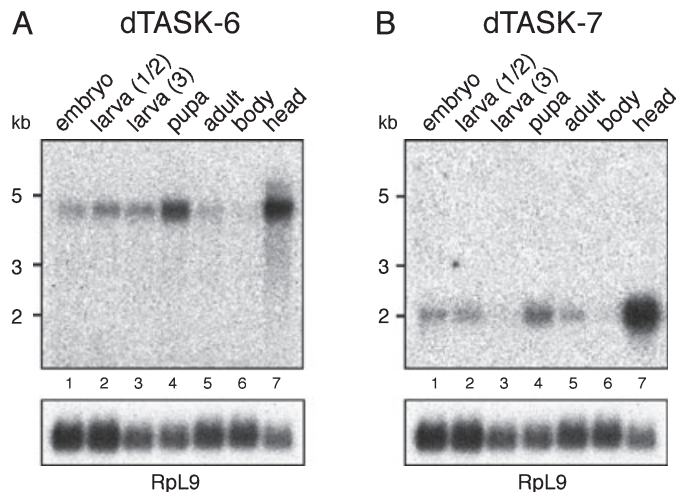


FIG. 2. Northern blot analysis dTASK channel expression in *Drosophila*. Blots containing 1 μg poly A⁺ RNA per lane were probed with ³²P-labeled antisense cRNA of dTASK-6 (A) and dTASK-7 (B). Samples in lanes 1 and 4 represent all embryonic and pupal stages, respectively, whereas larval developmental stages are further subdivided in first plus second (lane 2) and third (lane 3) instar larvae. In adult flies two-pore domain potassium channel expression was verified in either entire animals (lane 5) or fractions of body (lane 6) and head (lane 7). Probes detecting ribosomal protein RpL9 were used to normalize hybridization signals (bottom panels). The position of RNA size markers in kb is indicated on the left of A and B.

voltage clamp (data not shown). In contrast, currents measured in *Xenopus* oocytes after cRNA injection of dTASK-6, dTASK-7 or other cloned dK_{2P} channels were not significantly different from those of noninjected or water-injected oocytes ($n = 8$; data not shown).

As previously demonstrated, a specific cellular environment may be required for functional expression of channel proteins from *Drosophila* (Döring *et al.*, 2002). In *Drosophila* S2 cells weak signals of several dK_{2P} channel transcripts (*CG4296*, *CG10864*, *CG32770*, dTASK-6 and dTASK-7) were detected by reverse transcription-PCR (data not shown). When transfected with dTASK-6, whole-cell recordings upon voltage ramps from -150 to $+60$ mV in external medium containing 5.4 mM potassium gave rise to rapidly activating outward currents with a mean amplitude of 7.41 ± 4.05 nA ($n = 16$) at +30 mV which were absent in nontransfected cells (0.14 ± 0.07 nA at +30 mV, $n = 5$) (Fig. 4C). Elevating the extracellular K⁺ concentration shifted the reversal potential to more positive values as expected from the Nernst equation for K⁺-selective currents (-75 mV for 5.4 mM [K⁺]_e, -43 mV for 25 mM [K⁺]_e, -28 mV for 50 mM [K⁺]_e, -12 mV for 100 mM [K⁺]_e). In 100 mM extracellular K⁺ large inward currents could be recorded at negative membrane potentials, as predicted by the Goldman-Hodgkin-Katz current equation for a time- and voltage-independent leak K⁺ channel (Fig. 4A). The time course of current activation always measured in response to 500-ms voltage steps from -70 to $+80$ mV could be fitted by a single exponential with a time constant of 3.62 ± 2.24 ms ($n = 10$, Fig. 4C).

Except for ORK1, none of the other dK_{2P} channels induced measurable currents when transfected in S2 cells (data not shown). Whereas the failure of functional expression remained unclear for most K_{2P} channels, two nonconserved amino acids in the P1 domain of dTASK-7 (Ala92–Met93, Fig. 1B) appeared likely to be responsible for dysfunction. Thus, we substituted residues 92 and 93 in dTASK-7 by threonines that were highly conserved in every known K_{2P} channel at homologous positions. At 48 h after transfection of S2 cells with mutated dTASK-7 (dTASK-7^{AM92/93TT}), substantial outward currents similar to those of dTASK-6 were recorded. Mean current amplitudes

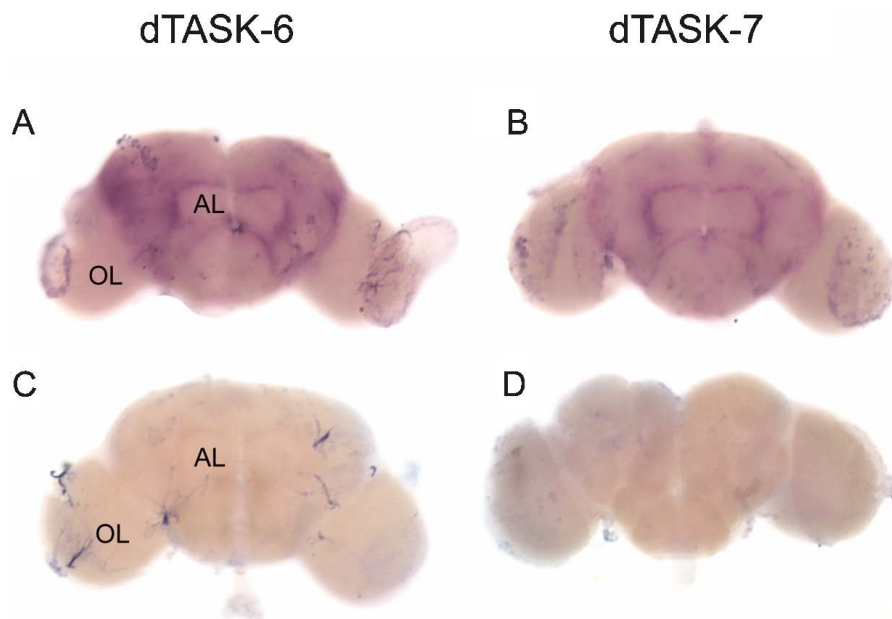


FIG. 3. Localization of dTASK-6 and dTASK-7 transcripts in the adult *Drosophila* brain. The expression of dTASK channels was analysed by whole-mount *in situ* hybridization with digoxigenin-labeled cRNA probes. Antisense probes of dTASK-6 (A) and dTASK-7 (B) revealed overlapping expression of both channels in the cortex of the antenna lobe (AL) but no transcripts were detected in the olfactory lobes (OL). Brain preparations hybridized with sense control cRNAs of dTASK-6 (C) and dTASK-7 (D) were not labeled.

of dTASK-7^{AM92/93TT} were 13.74 ± 3.75 nA at +30 mV ($n = 8$) with activation time constants of 2.96 ± 2.01 ms ($n = 8$, Fig. 4B and D).

Heteromerization of dTASK-6 and dTASK-7

Considering nonfunctional dTASK-7 homomers and neuronal colocalization of dTASK-6 and dTASK-7 (Fig. 3), we investigated the possibility that heteromeric dTASK channels may exist. Therefore, we initially cotransfected S2 cells with both wildtype dTASK subunits. In this case we measured K⁺ outward currents with decreased amplitudes (2.32 ± 1.29 nA at +30 mV, $n = 15$) compared with S2 cells transfected with dTASK-6 alone (current amplitude 7.41 ± 4.05 nA, $n = 16$; Student's *t*-test, $P < 0.001$). Putative coassembly of dTASK-6 and dTASK-7 could also be detected in the time course of current activation (Fig. 5). Depolarizing pulses elicited outward currents (Fig. 5A, upper left panel) with activation time constants clearly different from currents generated by dTASK-6 subunits alone (Fig. 4C). Current activation time constants of coexpressed dTASK-6 and dTASK-7 were almost fivefold slower ($\tau_{\text{on}} = 17.4 \pm 5.61$ ms, $n = 8$) than for homomeric dTASK-6 channels ($\tau_{\text{on}} = 3.62 \pm 2.24$ ms, $n = 10$). To investigate whether this difference resulted from heteromeric channels, concatemers of dTASK-6 and dTASK-7 were constructed. Following expression in S2 cells these constructs in fact elicited slowly activating outward currents ($\tau_{\text{on}} = 24.66 \pm 3.03$ ms, $n = 6$) with mean current amplitudes of 1.35 ± 1.01 nA at +30 mV ($n = 10$). Our observations (Fig. 5) strongly suggested that dTASK-6 and (nonfunctional) dTASK-7 subunits indeed formed heteromeric channel complexes.

Quite in contrast, mutant dTASK-7^{AM92/93TT} subunits, which were shown to give rise to fast activating K⁺ currents when transfected alone (Figs 4D and 5B), failed to slow down current activation in the concatemeric construct. When mutating the critical amino acids in the dTASK-6/7 concatemer (dTASK-6/7^{AM92/93TT}), currents remained rapidly activating with a time constant of 3.8 ± 1.45 ms ($n = 8$;

Fig. 5) and amplitudes were similar to homomeric dTASK channels (8.51 ± 2.28 nA, $n = 8$).

Acid sensitivity of *Drosophila* TASK channels

A prominent property of TASK channels is their dependency on external pH. Channel closure upon acidification was found to depend on an extracellular histidine conserved in all TASK channels (Rajan *et al.*, 2000; Lopes *et al.*, 2001). Following this rule, dTASK-6 displayed strong sensitivity to external proton concentrations. Changing the extracellular pH from 7.4 to 6.0 resulted in a complete but reversible loss of current activity (Fig. 6A). The pH dependence was extremely steep with a half-maximal inhibition at pH 6.8 (Fig. 6B).

Previously, a histidine at position 98 next to the GYG motif in the P1 region of TASK-3 was found to be responsible for pH sensitivity. Substitution of His-98 by an arginine in TASK-3 channels abolished their sensitivity to external acidification (Rajan *et al.*, 2000; Kim *et al.*, 2000). Accordingly, we mutated the homologous histidine in dTASK-6 to arginine and tested the pH sensitivity of the mutant (dTASK-6^{H98N}). Unexpectedly, dTASK-6^{H98N} was still pH-sensitive with an almost identical apparent pK of 6.85 (Fig. 6C–F). Similarly, mutation of a second extracellular histidine (His-72) to arginine (dTASK-6^{H72N}) generated currents that were still sensitive to external acidification in the same range as the dTASK-6 wildtype. Mutation of both putative proton sensors (H72N/H98N) resulted in a nonfunctional channel construct. The proton sensitivity of heteromeric dTASK-6/7 channels was identical to dTASK-6 homomers and was not affected by mutations at position 92/93 in dTASK-7 (data not shown).

Thus, an alternative pH sensing mechanism may be realized in dTASK channels. This is supported by our finding that the activity of dTASK-7^{AM92/93TT} harboring the same critical histidines (His-72 and His-98) was not dependent on extracellular acidification (Fig. 6E and F). In an attempt to transfer the pH sensor of dTASK-6 to the insensitive dTASK-7^{AM92/93TT} subunit we engineered chimeras between these two

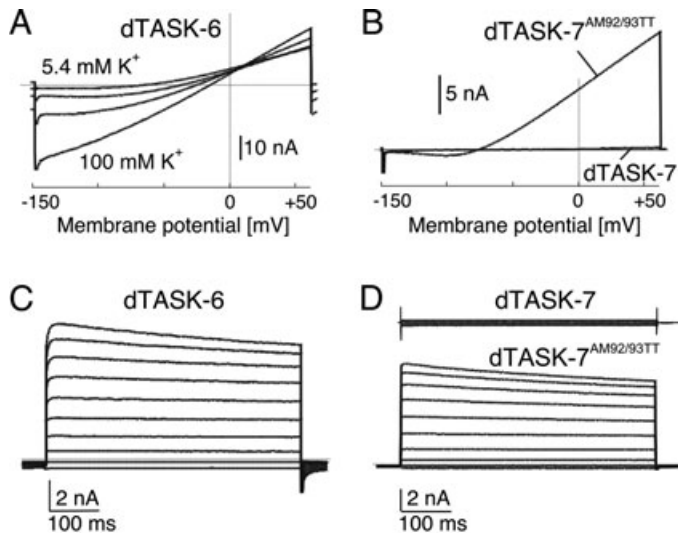


FIG. 4. Expression of dTASK channels in S2 cells. Whole-cell current recordings from S2 cells transfected with cDNA of dTASK-6 (A and C), dTASK-7 and dTASK-7^{AM92/93TT} (B and D). (A and B) Current-voltage relation in response to voltage ramps between -150 and +60 mV from a holding potential of -70 mV in 5.4 mM extracellular K⁺. In A currents of dTASK-6 were also recorded in 25, 50 and 100 mM external K⁺ replacing the equivalent sodium concentration. (C and D) Current recordings are shown in response to 500-ms voltage steps between -100 and +80 mV from a holding potential of -70 mV ([K⁺]_e = 5.4 mM). Transfected cells were identified by coexpressed enhanced green fluorescent protein.

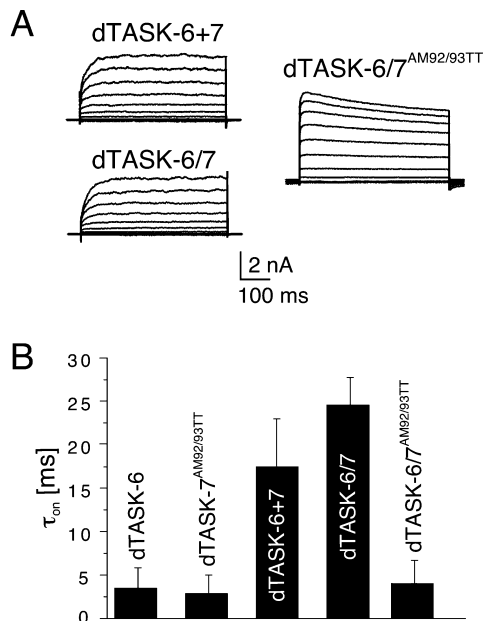


FIG. 5. Whole-cell currents and current activation time constants of homomeric and heteromeric dTASK channels. (A) Current recordings in response to 500-ms voltage steps between -100 and +80 mV from a holding potential of -70 mV ([K⁺]_e = 5.4 mM) from Schneider 2 (S2) cells cotransfected with dTASK-6 and dTASK-7 (upper left panel) or transfected with concatenated dTASK-6/7 (lower left panel) and dTASK-6/7^{AM92/93TT} (right panel). (B) Bar graph summarizing time constants from single exponentials fitted to current recordings (500 ms voltage step from -70 to +80 mV in 5.4 mM K⁺) from S2 cells transfected with dTASK-6, dTASK-7^{AM92/93TT}, concatenated dTASK-6/7 and dTASK-6/7^{AM92/93TT} or cotransfected with dTASK-6 and dTASK-7, respectively.

proteins. The N-terminus of dTASK-7^{AM92/93TT} including the entire (dTASK^{Chimera1}, exchange of Met¹-Ser⁸⁷) or partial (dTASK^{Chimera2}, Met¹-Val⁴⁹) extracellular loop between M1 and P1 was exchanged by the corresponding domains of dTASK-6 (indicated in Fig. 1B). Whereas dTASK^{Chimera1} was not expressed functionally, transfection of S2 cells with dTASK^{Chimera2} resulted in K⁺-selective currents that were inhibited by 78 ± 4% upon acidification from pH 7.4–6.0. Thus, with the first 49 amino acids of dTASK-6, proton sensitivity is partially transferred to dTASK-7^{AM92/93TT} (Fig. 6F). In the following we substituted five charged amino acids within this critical domain of dTASK-6 by noncharged or inversely charged residues in dTASK-7 (dTASK-6^{E32P}, dTASK-6^{K35A}, dTASK-6^{ED46/47KN}, dTASK-6^{E32P/K35A}, dTASK-6^{E32P-K35A-ED46/47KN} and dTASK-6^{E32P-K35A-ED46/47KN-D43T}). When transfected in S2 cells, all channel constructs elicited currents that were still inhibited by external acidification between 75 ± 13 and 98 ± 2%. In accordance with these findings the reverse chimera of dTASK^{Chimera2} with the first 49 amino acids of dTASK-6 replaced by the homologous domain of dTASK-7 (dTASK^{Chimera3}) was also inhibited by external acidification from pH 7.4–6.0 (88 ± 5%). In conclusion, it appears that the amino-terminus of dTASK-6 confers a partial pH sensitivity to dTASK-7^{AM92/93TT} but replacing this domain in dTASK-6 does not abolish its pH sensitivity. Thus, in addition to the 49 amino acids in the N-terminus another dominant pH-sensing region exists in dTASK-6. The distal extracellular M1-P1 loop may be a good candidate sensor but is not accessible to mutation analysis as documented by the nonfunctional dTASK^{Chimera1}.

Pharmacological properties of *Drosophila* TASK channels

To explore other characteristics that may help to discriminate between homomeric and heteromeric dTASK channels, we tested the effect of various pharmacological agents on currents evoked by dTASK-6 and dTASK-6/7 concatemers (Fig. 7).

Whole-cell current recordings from homomeric dTASK-6 or heteromeric dTASK-6/7 channels were resistant to inhibition by the classical K⁺ channel blocker Ba² (2 mM), when applied extracellularly. Bath application of the volatile anesthetic halothane (1 mM), known to activate mammalian TASK channels (Patel *et al.*, 1999), was also ineffective on both types of dTASK channels. Only weak current inhibition was observed with 20 μM anandamide (dTASK-6, -8 ± 5%; dTASK-6/7, -11 ± 4%) and 50 μM arachidonic acid (-25 ± 4%; -18 ± 3%) and no significant differences were found for homomeric and heteromeric dTASK channels. As inhibition by local anesthetics is characteristic for mammalian TASK-1 and TASK-3 (Kindler & Yost, 2005), we tested the effect of lidocaine (500 μM), bupivacaine (500 μM) and quinidine (100 μM) on the *Drosophila* orthologues. Whereas currents of homomeric dTASK-6 channels were substantially inhibited by these agents (bupivacaine, -87 ± 2%; quinidine, -80 ± 6%; lidocaine, -59 ± 5%), currents of dTASK-6/7 heteromers were resistant to quinidine and lidocaine and were inhibited by bupivacaine by only 38 ± 10% (Fig. 7). Thus, currents elicited by homomeric and heteromeric dTASK channels can be distinguished by the effects of local anesthetics, especially quinidine and lidocaine. To investigate the contribution of the Ala⁹² and Met⁹³ in dTASK-7 to the different sensitivity of homomeric and heteromeric dTASK channels, we analysed the corresponding mutants (dTASK-7^{AM92/93TT} and dTASK-6/7^{AM92/93TT}). When expressed alone, reduction of dTASK-7^{AM92/93TT} currents by local anesthetics (bupivacaine, -91 ± 2%; quinidine, -72 ± 6%; lidocaine, -57 ± 5%) was almost identical to current inhibition observed in homomeric dTASK-6 channels (see above). However, mutant dTASK-6/7^{AM92/93TT} concatemers were significantly more sensitive to local anesthetics

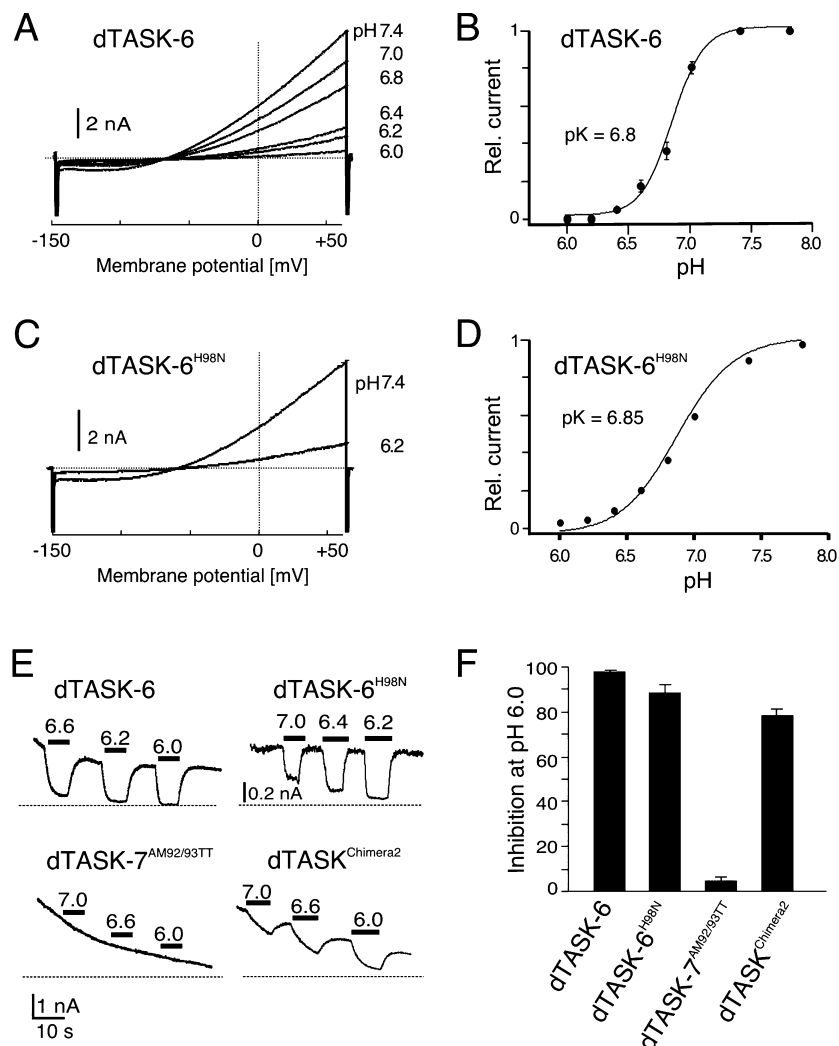


FIG. 6. Whole-cell current recordings from dTASK-transfected S2 cells at different pH. (A) Current recordings from S2 cells transfected with dTASK-6 in response to voltage ramps from -150 to $+60$ mV from a holding potential of -70 mV ($[K^+]_e = 5.4$ mM) at different pH. (B) pH-current response curve of dTASK-6 fitted by a Hill equation with an apparent pK of pH 6.8 and a Hill coefficient of 3.53. (C) Current recordings from S2 cells transfected with dTASK-6^{H98N} are shown in response to voltage ramps at pH 7.4 and 6.2. (D) pH-current response curve from cells transfected with dTASK-6^{H98N} (pK = 6.85). (E) Continuous recordings at a holding potential of $+30$ mV from cells transfected with dTASK-6, dTASK-6^{H98N}, dTASK-7^{AM92/93TT} and dTASK-7^{Chimera2} as depicted. The initial external pH of 7.4 was changed by application of extracellular solution with different pH as indicated by horizontal bars. (F) Bar graph showing current inhibition of wildtype and mutated dTASK channels upon exchange of external proton concentration from pH 7.4 to 6.0. Values for relative current inhibition are the mean \pm SD of five individual measurements.

(bupivacaine, $-58 \pm 5\%$; quinidine, $-24 \pm 5\%$; lidocaine, $-16 \pm 4\%$) than wildtype heteromers (dTASK-6/7). The sensitivity for quinidine and lidocaine was increased three- and eightfold, respectively, indicating an important influence of pore loop residues Ala⁹² and Met⁹³ on these specific pharmacological properties of heteromeric dTASK channels.

Finally, as dTASK-6 and dTASK-7 subunits harbor various putative PKA phosphorylation sites (Fig. 1B), we also looked for current modulation by PKA activation with forskolin. Extracellular application of $50 \mu\text{M}$ forskolin reduced currents of dTASK-6 homomers and dTASK-6/7 heteromers by 88 ± 3 and $87 \pm 4\%$, respectively.

Discussion

Two novel *Drosophila* TASK subunits are functionally expressed in S2 cells

In the *Drosophila* genome, 10 putative gene products were identified that share typical structural features of mammalian K_{2P} channels.

Previously, 11 members of the K_{2P} family have been predicted from the *Drosophila* genome (Littleton & Ganetzky, 2000). However, the questionable gene product (*CG3367*; Drysdale *et al.*, 2005) does indeed have significant sequence similarity to K_{2P} subunits but lacks a second pore domain matching the canonical pore signature (TT[IV]-G[YF]G). Two dK_{2P} subunits display profound sequence similarity to human TASK subunits (between 38 and 45%) and thus were named dTASK-6 and dTASK-7. In contrast, all other dK_{2P} subunits are located on a separate branch of the phylogenetic tree (Fig. 1A). A similar situation is present in the *Caenorhabditis elegans* genome where among ~ 50 different K_{2P} genes only two TASK-like subunits (n2P20 and n2P38) show significant homology to mammalian K_{2P} channels (Salkoff *et al.*, 2001). Among few reports describing functional aspects of K_{2P} channel genes in *C. elegans* (e.g. Kunkel *et al.*, 2000), a genetic study demonstrated that TASK gene n2P38 (or sup-9) is involved in coordination of muscle contraction in the worm (Perez del la Cruz *et al.*, 2003). Nevertheless, in *Drosophila* functional properties of TASK channels are still unknown (Buckingham *et al.*, 2005).

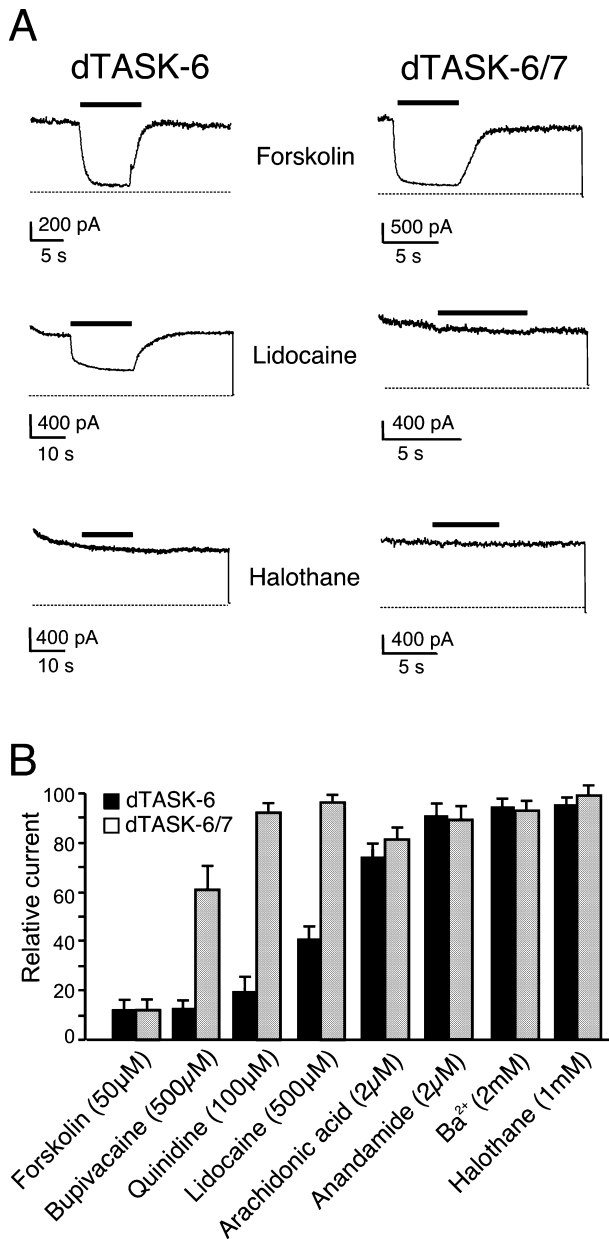


FIG. 7. Pharmacological modulation of dTASK-6 and dTASK-6/7 channels. (A) Continuous recordings at a holding potential of +30 mV from Schneider 2 cells transfected with dTASK-6 (left) and dTASK-6/7 (right) upon application of forskolin (50 μM, upper traces), lidocaine (500 μM, middle traces) and halothane (1 mM, lower traces) as indicated by horizontal bars. (B) Bar graph showing the effects of different agents on the activity of dTASK-6 (black bars) and dTASK-6/7 concatemers (grey bars). Relative current values are the mean ± SD of six to eight individual measurements.

As reported before for *Drosophila* Kir channels (Döring *et al.*, 2002), the majority of dK_{2P} channels failed to functionally express in *Xenopus* oocytes. Fortunately, *Drosophila* S2 cells were found to provide a suitable cellular environment for dTASK-6 and dTASK-7, as well as for numerous insect ion channels and receptors (Towers & Sattelle, 2002).

Functional expression of dTASK-7 subunits was observed only after introducing mutations in the P1 domain. The exchange of a unique Ala-Met doublet near the pore selectivity filter (dTASK-

7^{AM92/93TT}) was sufficient to evoke typical TASK currents in S2 cells. As expected from the primary sequence, the existence of functional channels from wildtype dTASK-7 subunits was unlikely because a threonine at position -2 relative to the GYG motif (TT[IV]GYG) is highly conserved in all potassium channels and was shown to line the ion-conductance pathway (Doyle *et al.*, 1998). The threonine at position -3 is less conserved and sometimes exchanged by serine, leucine or valine. Apparently substitutions in this region interfere with the proper structure of a K⁺-selective channel.

Colocalized dTASK-6 and dTASK-7 assemble into heteromeric channels with unique functional properties

Neuronal expression of both dTASK subunits is evident from northern blots revealing strong RNA signals in the head of adult fruit flies. As demonstrated by whole-mount brain *in situ* hybridizations dTASK-6 and dTASK-7 display overlapping expression patterns in the antennal lobes and thus may form heteromeric channels in *Drosophila* neurons.

The ability of closely related K⁺ channel subunits to associate into functional heteromeric channels is well established within the voltage-gated and inwardly-rectifying K⁺ channel families (Krapivinsky *et al.*, 1995; Wang *et al.*, 1998). Recently, the formation of heteromeric channels comprising subunits of the K_{2P} channel family was reported. Heteromers of mammalian TASK-1 and TASK-3 were identified when expressed in heterologous systems as well as in native tissues. However, in the current analysis homomeric and heteromeric channels were distinguishable only by moderate differences in their sensitivity to isoflurane, ruthenium red and protons (Czirják & Enyedi, 2002; Kang *et al.*, 2003; Berg *et al.*, 2004).

Here we demonstrate that dTASK-6 and dTASK-7 subunits coexpressed in S2 cells can form heteromeric channels with reduced current amplitudes, significantly slower current activation kinetics and weaker sensitivity to local anesthetics (see below) compared with dTASK homomers.

Several mammalian K_{2P} isoforms (TASK-5, THIK-2, TWIK-1 and KCNK-7) have been found to be inadequately expressed in recombinant systems (Karschin *et al.*, 2001; Salinas *et al.*, 1999; Rajan *et al.*, 2001). This may result from improper targeting to the plasma membrane (Karschin *et al.*, 2001), post-translational modifications (Rajan *et al.*, 2005) or down-regulation by as yet unknown mechanisms (Salinas *et al.*, 1999; Rajan *et al.*, 2001). In coexpression studies no evidence was found for these nonfunctional subunits to regulate closely related subfamily members (e.g. Rajan *et al.*, 2001; Ashmole *et al.*, 2001; Karschin *et al.*, 2001).

When individually expressed in *Drosophila* S2 cells dTASK-7 does not evoke measurable currents although, in association with dTASK-6, acid-sensitive channels with distinct functional properties were formed. Macroscopic currents derived from coexpressed and concatenated dTASK-6 and dTASK-7 subunits displayed similar electrophysiological characteristics. Somewhat higher current amplitudes and faster activation kinetics when subunits were coexpressed probably result from a mixture of homomeric dTASK-6 and heteromeric dTASK-6/7 channels which were not resolved by whole-cell current measurements. As revealed by mutated dTASK-6/7 concatemers (dTASK-6/7^{AM92/93TT}), the two amino acids (Ala92-Met93) in P1 that prevent the formation of functional dTASK-7 homomers induce altered conductance properties of the heteromeric channel.

G protein-activated Kir channels provide another example where homomeric channels are only poorly assembled. In the pore region of

Kir3.1, a bulky phenylalanine (Phe137) may prevent homomeric assembly but favors a combination with Kir3.2–3.4 subunits. In addition, the nonconserved phenylalanine in the pore loop of Kir3.1 was shown to control current amplitude and gating of heteromeric Kir3 channels (Chan *et al.*, 1996; Wischmeyer *et al.*, 1997).

In the family of K_{2P} channels, dTASK-7 is the first subunit that does not form functional channels on its own but instead efficiently assembles into dTASK-6/7 heteromers to alter the channel properties by unique structural elements. Colocalization of dTASK-6 and dTASK-7 subunits in *Drosophila* neurons may generate functionally different acid-sensitive leak K^+ currents *in vivo*.

Proton sensitivity and pharmacological properties of *Drosophila* TASK channels

A key property of TASK channels is their sensitivity to changes in external pH in the physiological range. Whole-cell currents measured in S2 cells transfected with dTASK-6 decrease with extracellular acidification. dTASK-6 channels were enhanced or inhibited within a range of 0.8 pH units around extracellular H^+ changes between pH 6.5 and 7.3 (pK 6.8). A similar proton sensitivity near physiological pH has been reported for human TASK-1 (Duprat *et al.*, 1997; pK 7.3) and rat TASK-3 (Kim *et al.*, 2000; pK 6.7). Whereas in mammals the mutation of conserved histidine 98 to asparagine almost completely abolished proton sensitivity (Kim *et al.*, 2000; Rajan *et al.*, 2000; Lopes *et al.*, 2001), the homologous mutation in dTASK-6 had almost no effect. We also reveal that currents evoked by dTASK-7^{AM92/93TT} (with His98) were not affected by changes in external pH and therefore hypothesize the existence of an alternative pH sensor in dTASK channels. Proton sensitivity of a chimera between dTASK-6 and dTASK-7^{AM92/93TT} (dTASK^{Chimera2}) indicated the first 49 amino acids of dTASK-6 as a proton-sensing domain. However, as the reverse chimeric construct (dTASK^{Chimera3}) was still acid sensitive we propose the existence of a second pH-sensitive element in dTASK-6. As the extracellular region between M3 and P2 is highly conserved, an additional pH sensor is more likely to be located in the distal part of the extracellular M1-P1 loop. Unfortunately, domain swapping in this region resulted in nonfunctional channels.

It is evident from the identical pH sensitivity of homomeric dTASK-6 and heteromeric dTASK-6/7 channels that a single pH-sensitive subunit is sufficient to render the entire channel vulnerable to extracellular protons. Our study with *Drosophila* TASK orthologues suggests an alternative pH-sensing mechanism independent of extracellular histidines. Similarly, human TASK-2 channels (TALK subfamily, Fig. 1A) are also sensitive to extracellular pH although the histidine next to the GYG motif is replaced by an asparagine (Reyes *et al.*, 1998). A network of charged residues in the M1–P1 loop was recently identified in murine TASK-2 subunits acting as an alternative pH sensor (Morton *et al.*, 2005).

Within the TASK channel subfamily, six conserved amino acids (VLR[F/M/L]T) were found to be a key structural element conferring regulation by G protein-coupled receptors ($G_{q/11}$) and volatile anesthetics. Activation of mammalian TASK-1 channels by halothane strictly depends on the presence of the VLR[F/M/L]T motif and the effect seems to be independent of intracellular second messengers (Patel *et al.*, 1999; Talley & Bayliss, 2002). Although the critical motif distal to transmembrane segment M4 is also present in dTASK-6 and dTASK-7 (compare Fig. 1B), neither homomeric dTASK-6 nor heteromeric dTASK-6/7 channels responded to extracellular application of halothane. Apparently, the VLR[F/M/L]T motif is not sufficient to confer halothane sensitivity but other

structural elements are necessary to activate TASK channels by halothane. There is additional evidence that the halothane interaction with the channel may be quite variable. Mammalian TASK-3 channels are still activated by halothane although the VLRFLT motif was deleted (unpublished observation) and in TREK-1 a completely different C-terminal region is critical for channel activation by halothane (Patel *et al.*, 1999).

Polyunsaturated fatty acids, including arachidonic acid and anandamide, are signaling molecules that modulate the activity of mammalian K_{2P} channels. Whereas TREK currents are increased several fold by arachidonic acid, the activity of mammalian TASK channels is inhibited between 60 and 70% (Kim *et al.*, 2000; Lopes *et al.*, 2000). The endocannabinoid anandamide modulates members of the TASK subfamily more specifically. At micromolar concentrations, TASK-1 and TASK-3 currents are inhibited by 90 and 50%, respectively (Maingret *et al.*, 2001). Although the primary sequences of mammalian and *Drosophila* TASK subunits are very similar, no effect of anandamide and only a weak current inhibition by arachidonic acid were observed in fly orthologues.

As mammalian TASK-1 and TASK-3 currents are inhibited by local anesthetics such as bupivacaine, lidocaine and quinidine (also an antiarrhythmic drug) in the 100- μ M range (Leonoudakis *et al.*, 1998; Kim *et al.*, 2000; Meadows & Randall, 2001), we tested the effect of these agents on currents of dTASK-6 homomers and dTASK-6/7 heteromers. All substances were profound inhibitors of homomeric dTASK-6 currents but were ineffective (lidocaine and quinidine) or less effective (bupivacaine) on currents of heteromeric dTASK-6/7 channels. Differences were most prominent for quinidine (100 μ M) which blocks dTASK-6 by 80% and dTASK-6/7 by only 7%. We found an increased sensitivity of mutated dTASK-6/7^{AM92/93TT} (24% inhibition), suggesting that pore loop residues Ala92–Met93 in dTASK-7 are also important structural determinants for the discrepancy in pharmacological properties of dTASK-6 and dTASK-6/7. Thus, in addition to different current activation kinetics and current amplitudes, homomeric and heteromeric dTASK channels are distinguishable by their variable sensitivity to local anesthetics, especially quinidine.

Using forskolin as an activator of adenylyl cyclase we investigated the coupling of dTASK channels to the cAMP signaling pathway. An intracellular increase of cAMP by forskolin (50 μ M) inhibited homomeric and heteromeric dTASK currents by almost 90%. This effect may result from PKA phosphorylation of several consensus sites in the primary sequence of dTASK-6 and dTASK-7 (Fig. 1B). In *Drosophila*, cAMP signaling was found to be particularly important for olfactory memory formation. Many mutants impaired in olfactory learning have mutations in genes that encode components of the cAMP signaling pathway, e.g. *rutabaga* (adenylyl cyclase) or *dunce* (cAMP-specific diesterase). In addition, genetically reduced expression of PKA or cAMP response element binding protein, a transcription factor stimulated by PKA, impairs short- or long-term memory, respectively (reviewed by Davis, 2005).

In the marine snail *Aplysia* behavioral sensitization is regulated similarly by cAMP signaling. This form of simple learning underlies presynaptic facilitation of transmitter release which is controlled by serotonin-sensitive S-type background K^+ channels (Siegelbaum *et al.*, 1982; Hawkins *et al.*, 1993). S-type K^+ channels sharing several properties with members of the K_{2P} channel family, e.g. leak K^+ conductance or direct activation by volatile anesthetics (Winegar & Yost, 1998) are closed by cAMP-dependent phosphorylation via PKA (Shuster *et al.*, 1985). Therefore, in *Drosophila*, d K_{2P} channels may also play a role in olfactory learning.

Acknowledgements

We thank B. Trost, M. Oppmann, T. Martini and H. Lorentz for excellent technical assistance. We are grateful to C. Smith for his comments on the manuscript.

Abbreviations

K_{2P}, two-pore domain potassium; dK_{2P}, *Drosophila* K_{2P}; KCNK, potassium (K_{2P}) channel subunits; TASK, TWIK-related acid-sensitive K⁺; dTASK, *Drosophila* TWIK-related acid-sensitive K⁺; ORF, open reading frame; PCR, polymerase chain reaction; PKA, protein kinase A; S2, Schneider 2.

References

- Adams, M.D., Celniker, S.E., Holt, R.A. et al. (2000) The genome sequence of *Drosophila melanogaster*. *Science*, **287**, 2185–2195.
- Ashmole, I., Goodwin, P.A. & Stanfield, P.R. (2001) TASK-5, a novel member of the tandem pore K⁺ channel family. *Pflügers Arch.*, **442**, 828–833.
- Bayliss, D.A., Sirios, J.E., Talley & E.M. (2003) The TASK family: two-pore domain background K⁺ channels. *Mol. Interv.*, **3**, 205–219.
- Berg, A.P., Talley, E.M., Manger, J.P. & Bayliss, D.A. (2004) Motoneurons express heteromeric TWIK-related acid-sensitive K⁺ (TASK) channels containing TASK-1 (KCNK3) and TASK-3 (KCNK9) subunits. *J. Neurosci.*, **24**, 6693–6702.
- Buckingham, S.D., Kidd, J.F., Law, R.J., Franks, C.J. & Sattelle, D.B. (2005) Structure and function of two-pore-domain K⁺ channels: contribution from genetic model organisms. *Trends Pharmacol. Sci.*, **26**, 361–367.
- Chan, K.W., Sui, J.-L., Vivaudou, M. & Logothetis, D.E. (1996) Control of channel activity through a unique amino acid residue of a G protein-gated inwardly rectifying K⁺ channel subunit. *Proc. Natl Acad. Sci. U.S.A.*, **93**, 14 193–14 198.
- Czirják, G. & Enyedi, P. (2002) Formation of functional heterodimers between the TASK-1 and TASK-3 two-pore domain potassium channel subunit. *J. Biol. Chem.*, **277**, 5426–5432.
- Davis, R.L. (2005) Olfactory memory formation in *Drosophila*: from molecular to systems neuroscience. *Annu. Rev. Neurosci.*, **28**, 275–302.
- Döring, F., Wischmeyer, E., Kühnlein, R.P., Jäckle, H. & Karschin, A. (2002) Inwardly rectifying K⁺ (Kir) channels in *Drosophila*. A crucial role of cellular milieu factors for Kir channel function. *J. Biol. Chem.*, **277**, 25 554–25 561.
- Doyle, A.D., Carbral, J.M., Pfuetzner, R.A., Kuo, A., Gulbis, J.M., Cohen, S.L., Chait, B.T. & MacKinnon, R. (1998) The structure of the potassium channel: Molecular basis of K⁺ conduction and selectivity. *Science*, **280**, 69–77.
- Drysdale, R.A., Crosby, M.A. & the FlyBase Consortium (2005) FlyBase: genes and gene models. *Nucl. Acids Res.*, **33**, D390–D395. <http://flybase.org/>.
- Duprat, F., Lesage, F., Fink, M., Reyes, R., Heurteaux, C. & Lazdunski, M. (1997) TASK, a human background K⁺ channel to sense external variations near physiological pH. *EMBO J.*, **17**, 5464–5471.
- Goldstein, S.A.N., Price, L.A., Rosenthal, D.N. & Pausch, M.A. (1996) ORK1, a potassium-selective leak channel with two pore domains cloned from *Drosophila melanogaster* by expression in *Saccharomyces cerevisiae*. *Proc. Natl Acad. Sci. U.S.A.*, **93**, 13 256–13 261.
- Goldstein, S.A.N., Bockenhauer, D., O'Kelly, I. & Zilberberg, N. (2001) Potassium channels and the KCNK family of two-P-domain subunits. *Nat. Rev. Neurosci.*, **2**, 175–184.
- Hawkins, R.D., Kandel, E.R. & Siegelbaum, S.A. (1993) Learning to modulate transmitter release: themes and variations in synaptic plasticity. *Annu. Rev. Neurosci.*, **16**, 625–665.
- Horton, R.M., Hunt, H.D., Ho, S.N., Pullen, J.K. & Pease, L.R. (1989) Engineering hybrid genes without the use of restriction enzymes: gene splicing by overlap extension. *Gene*, **77**, 61–68.
- Kang, D., Han, J., Talley, E.M., Bayliss, D.A. & Kim, D. (2003) Functional expression of TASK-1/TASK-3 heteromers in cerebellar granule cells. *J. Physiol.*, **554**, 64–77.
- Karschin, C., Wischmeyer, E., Preisig-Müller, R., Rajan, S., Derst, C., Grzeschik, K.-H., Daut, J. & Karschin, A. (2001) Expression pattern in brain of TASK-1, TASK-3, and a tandem pore domain K⁺ channel subunit, TASK-5, associated with the central auditory nervous system. *Mol. Cell. Neurosci.*, **18**, 632–648.
- Kim, Y., Bang, H. & Kim, D. (2000) TASK-3 a new member of the tandem pore K⁺ channel family. *J. Biol. Chem.*, **275**, 9340–9347.
- Kindler, C.H. & Yost, C.S. (2005) Two-pore domain potassium channels: new sites of local anesthetic action and toxicity. *Region. Anesth.*, **30**, 260–274.
- Krapivinsky, G., Gordon, E.A., Wickman, K., Velimirovic, B., Krapivinsky, L. & Clapham, D.E. (1995) The G-protein-gated atrial K⁺ channel IK_{ACh} is a heteromultimer of two inwardly rectifying K⁺-channel proteins. *Nature*, **374**, 135–141.
- Kunkel, M.T., Duncan, B.J., Thomas, J.H. & Salkoff, L. (2000) Mutants of temperature-sensitive two-P domain potassium channel. *J. Neurosci.*, **20**, 7517–7524.
- Leonoudakis, D., Gray, A.T., Winegar, B.D., Kindler, C.H., Harada, M., Taylor, D.M., Chavaz, R.A., Forsayeth, J.R. & Yost, C.S. (1998) An open rectifier potassium channel with two pore domains in tandem cloned from rat cerebellum. *J. Neurosci.*, **18**, 868–877.
- Littleton, J.T. & Ganetzky, B. (2000) Ion channels and synaptic organisation: Analysis of the *Drosophila* genome. *Neuron*, **26**, 35–43.
- Lopes, C.E.B., Gallagher, P.G., Buck, M.E., Butler, M.H. & Goldstein, S.A.N. (2000) Proton block and voltage gating are potassium-dependent in the cardiac leak channel Kcnk3. *J. Biol. Chem.*, **275**, 19 969–16 978.
- Lopes, C.M.B., Zilberberg, N. & Goldstein, S.A.N. (2001) Block of Kcnk3 by protons. Evidence that 2-P-domain potassium channel subunits function as homodimers. *J. Biol. Chem.*, **276**, 24 449–244 520.
- Maingret, F., Patel, A.J., Lazdunski, M. & Honoré, E. (2001) The endocannabinoid anandamide is a direct and selective blocker of the background K⁺ channel TASK-1. *EMBO J.*, **20**, 47–54.
- Meadows, H.J. & Randall, A.D. (2001) Functional characterization of human TASK-3, an acid-sensitive two-pore domain potassium channel. *Neuropharmacology*, **40**, 551–559.
- Medhurst, A.D., Rennie, G., Chapman, C.G., Meadows, H., Duckworth, M.D., Kelsell, R.E., Gloger, I.I. & Pangalos, M.N. (2001) Distribution analysis of human two pore domain potassium channels in tissues of the central nervous system and periphery. *Mol. Brain Res.*, **86**, 101–114.
- Methfessel, C., Witzemann, V., Takashi, T., Mishina, M., Numa, S. & Sakmann, B. (1986) Patch-clamp measurements on *Xenopus* oocytes: currents through endogenous channels and implanted acetylcholine receptor and sodium channels. *Pflügers Arch.*, **407**, 577–588.
- Morton, M.J., Abohamed, A., Sivaprasadarao, A. & Hunter, M. (2005) pH sensing in the two-pore domain K⁺ channel, TASK2. *Proc. Natl Acad. Sci. U.S.A.*, **102**, 16 102–16 106.
- Patel, A.J. & Honoré, E. (2001) Properties and modulation of mammalian 2P domain K⁺ channels. *Trends Neurosci.*, **24**, 339–346.
- Patel, A.J., Honoré, E., Lesage, F., Fink, M., Romey, G. & Lazdunski, M. (1999) Inhalational anesthetics activate two-pore-domain background K⁺ channels. *Nat. Neurosci.*, **2**, 422–426.
- Perez del la Cruz, I., Levin, J.Z., Cummins, C., Anderson, P. & Horvitz, H.R. (2003) sup-9, sup-10, and unc93 may encode components of a two pore K⁺ channel that coordinates muscle contraction in *Caenorhabditis elegans*. *J. Neurosci.*, **27**, 9133–9145.
- Rajan, S., Wischmeyer, E., Liu, G.X., Preisig-Müller, R., Daut, J., Karschin, A. & Derst, C. (2000) TASK-3, a novel tandem pore domain acid-sensitive K⁺ channel. *J. Biol. Chem.*, **275**, 16 650–16 657.
- Rajan, S., Wischmeyer, E., Karschin, C., Preisig-Müller, R., Grzeschik, K.-H., Daut, J., Karschin, A. & Derst, C. (2001) THIK-1 and THIK-2, a novel subfamily of tandem pore domain K⁺ channels. *J. Biol. Chem.*, **276**, 7302–7311.
- Rajan, S., Plant, L.D., Rabin, M.L., Butler, M.H. & Goldstein, S.A.M. (2005) Sumoylation silences the plasma membrane leak K⁺ channel K2P1. *Cell*, **121**, 37–47.
- Reyes, R., Duprat, F., Lesage, F., Fink, M., Salinas, M., Farman, N. & Lazdunski, M. (1998) Cloning and expression of a novel pH-sensitive two pore domain K⁺ channel from human kidney. *J. Biol. Chem.*, **273**, 30 863–30 869.
- Salinas, M., Reyes, R., Lesage, F., Fosset, M., Heurteaux, C., Romey, G. & Lazdunski, M. (1999) Cloning of a new mouse two-P domain channel subunit and a human homologue with a unique pore structure. *J. Biol. Chem.*, **274**, 11 751–11 760.
- Salkoff, L., Butler, A., Fawcett, G., Kunkel, M., McArdale, C., Paz-Y-Mino, G., Nonet, M., Walton, N., Wang, Z.-W., Yuan, A. & Wei, A. (2001) Evolution tunes the excitability of individual neurons. *Neuroscience*, **103**, 853–859.
- Sano, Y., Inamura, K., Miyake, A., Mochizuki, S., Kitada, C., Yokoi, H., Nozawa, K., Okada, H., Matsushime, H. & Furuichi, K. (2003) A novel two-pore domain K⁺ channel, TRESK, is localized in the spinal cord. *J. Biol. Chem.*, **278**, 27 406–27 412.
- Schmidt, A., Hollmann, A. & Schäfer, U. (1996) A newly identified minute locus, M(2)32D, encodes the ribosomal protein L9 in *Drosophila melanogaster*. *Mol. Gen. Genet.*, **251**, 381–387.
- Schneider, I. (1972) Cell lines derived from late embryonic stages of *Drosophila melanogaster*. *J. Embryol. Exp. Morphol.*, **27**, 363–365.

- Shuster, M.J., Camardo, J.S., Siegelbaum, S.A. & Kandel, E.R. (1985) Cyclic AMP-dependent protein kinase closes serotonin-sensitive K⁺ channels in *Aplysia* sensory neurons in cell-free membrane patches. *Nature*, **313**, 392–395.
- Siegelbaum, S.A., Camardo, J.S. & Kandel, E.R. (1982) Serotonin and cyclic AMP close single K⁺ channels in *Aplysia* sensory neurons. *Nature*, **299**, 413–417.
- Talley, E.M. & Bayliss, D.A. (2002) Modulation of TASK-1 (Kcnk3) and TASK-3 (Kcnk9) potassium channels. *J. Biol. Chem.*, **277**, 17 733–17 742.
- Tautz, D. & Pfeifle, C. (1989) A non-radioactive *in situ* hybridization method for the localization of specific RNAs in *Drosophila* embryos reveals translational control of the segmentation gene hunchback. *Chromosoma*, **98**, 81–85.
- Towers, P.R. & Sattelle, D.B. (2002) A *Drosophila melanogaster* cell line (S2) facilitates post-genome functional analysis of receptors and ion channels. *Bioessays*, **24**, 1066–1073.
- Wang, H.S., Pan, Z., Shi, W., Brown, B.S., Wymore, R.S., Cohen, I.S., Dixon, J.E. & MacKinnon, D. (1998) KCNQ2 and KCNQ3 potassium channel subunits: molecular correlates of the M-channel. *Science*, **282**, 1890–1893.
- Winegar, B.D. & Yost, C.S. (1998) Volatile anesthetics directly activate baseline S K⁺ channels in *Aplysia* neurons. *Brain Res.*, **807**, 255–262.
- Wischmeyer, E., Döring, F., Wischmeyer, E., Spauschus, A., Thomzig, A., Veh, R. & Karschin, A. (1997) Subunit interactions in the assembly of neuronal Kir3.0 inwardly rectifying K⁺ channels. *Mol. Cell. Neurosci.*, **9**, 194–206.